Available online at www.sciencedirect.com
SCIENCE DIRECT®
Coordination Chemistry Reviews 245 (2003) 73–83
COORDINATION CHEMISTRY REVIEWS
www.elsevier.com/locate/ccr

Coordination and release of NO by ruthenium–dimethylsulfoxide complexes—implications for antimetastases activity

Barbara Serli [a], Ennio Zangrando [a], Teresa Gianferrara [b], Lesley Yellowlees [c], Enzo Alessio [a,*]

[a] *Dipartimento di Scienze Chimiche, Università di Trieste, Trieste 34127, Italy*
[b] *Dipartimento di Scienze Farmaceutiche, Università di Trieste, Trieste 34127, Italy*
[c] *Department of Chemistry, University of Edinburgh, Edinburgh EH9 3JJ, UK*

Received 16 October 2002; accepted 14 March 2003

Contents

Abstract

Several Ru(II) and Ru(III)–dimethylsulfoxide (DMSO) complexes, that are not cytotoxic in vitro, are endowed with anticancer and, in particular, antimetastatic activity against animal tumor models. One possibility for explaining the activity of such compounds against disseminated tumors is that they interfere with NO metabolism in vivo. Thus, we investigated the reactivity of ruthenium–chloride–DMSO complexes towards NO with the aim of producing well-characterized models to be used as reference compounds in subsequent biomimetic studies. In this contribution, we report on the synthesis, spectroscopic, structural and electrochemical characterization of anionic (e.g. $[(DMSO)_2H][$*trans*-$RuCl_4(DMSO\text{-}O)(NO)]$ (**1**)), neutral (e.g. *mer*,*cis*-$RuCl_3(DMSO\text{-}O)_2(NO)$ (**2**)) and new cationic (e.g. [*cis*,*fac*-$RuCl_2(DMSO\text{-}O)_3(NO)][BF_4]$ (**9**)) Ru–DMSO nitrosyls, derived from both Ru(II) and Ru(III)–chloride–DMSO precursors. Coordination of the strong π-acceptor NO favors coordination of DMSO ligands through oxygen (DMSO-O) to avoid competition for π electrons. The reactivity of some Ru–DMSO–NO complexes towards heterocyclic N-ligands, leading to compounds such as $[(Im)_2H][$*trans*-$RuCl_4(Im)(NO)]$ (Im = imidazole, **6**) and [*cis*,*mer*-$RuCl_2(py)_3(NO)][BF_4]$ (py = pyridine, **10**), is also described. The spectroscopic and X-ray structural features for all these complexes are consistent with the $\{Ru(NO)\}^6$ formulation, that is a diamagnetic Ru(II) nucleus bound to NO^+. Electrochemical

* Corresponding author. Tel.: +39-040-5583961; fax: +39-040-5583903.
E-mail address: alessi@univ.trieste.it (E. Alessio).

0010-8545/$ – see front matter © 2003 Elsevier B.V. All rights reserved.
doi:10.1016/S0010-8545(03)00056-0

measurements on the Ru–NO complexes showed that they are all redox active in DMF solutions and the site of reduction is the NO^+ moiety. With the exception of **10**, the reduced complexes are not stable and rapidly release the $NO^\bullet$ radical.
© 2003 Elsevier B.V. All rights reserved.

Keywords: Ruthenium; Dimethylsulfoxide; Nitrosyl; NO-releasing agents; Anticancer

1. Introduction

The high affinity of ruthenium for NO is well documented [1]. Compounds of this metal with readily available coordination sites are being investigated as NO scavengers (e.g. for the treatment of septic shock) [2]. On the other hand, ruthenium nitrosyl complexes are investigated as controlled NO-releasing agents for medicinal applications [3,4], in particular for the control of high blood pressure (vasodilatation), and as antitumor agents which might release cytotoxic NO within tumor cells, thus leading to cell death. Most octahedral ruthenium-nitrosyls feature the linear $\{Ru(NO)\}^6$ moiety, that is a diamagnetic Ru(II) center bound to NO^+ [5]. Modulation of NO release can be induced by one-electron reduction [3], which occurs at the NO^+ to yield coordinated $NO^\bullet$, or by photolysis [4].

In the last few years we prepared several Ru(II) and Ru(III)–dimethylsulfoxide (DMSO) complexes that are not cytotoxic in vitro but are nevertheless endowed with anticancer activity against animal tumor models [6]. One such compound, [ImH][*trans*-$RuCl_4$(DMSO-S)(Im)] (NAMI-A, Im = imidazole), while not particularly active against the growth of primary tumor, is very effective in selectively inhibiting the formation and growth of spontaneous metastases [7]; for this reason, in 1999 NAMI-A was introduced into phase I clinical trials.

The low cytotoxicity of NAMI-A and related Ru–DMSO complexes suggests that their primary mechanism of action is different from that of cytostatic Pt drugs and might be unrelated to interactions with DNA [8]. One possibility for explaining the activity of NAMI-A against disseminated tumors is that it interferes with NO metabolism in vivo. Nitric oxide is known to play an important role in many biological functions [9] and recently it was demonstrated to be involved as mediator in one tumor-induced angiogenic process, which is a key step in the formation of metastases [10]. NO is also known to interact in vivo with iron proteins [11]; thus, ruthenium action might also occur through an iron-mimicking mechanism.

Within this general framework we previously reported the reactivity of Ru(II) and Ru(III)–chloride–DMSO complexes and of NAMI-A towards NO and reactions of the resulting nitrosyls with heterocyclic N-ligands to give spectroscopically and structurally well-characterized models (**1**–**8**) (Schemes 1–6) [12]. We report in this article on the further characterization of some of these and on the synthesis, spectroscopic, structural and electrochemical characterization of several new complexes. These will be used as reference compounds in subsequent biomimetic studies in physiological conditions aimed to understand whether the antimetastases activity of some ruthenium–DMSO complexes might be due to their in vivo interactions with NO.

2. Experimental

Compounds **1**–**8** were prepared according to the procedures already described by us [12,13]. UV–vis spectra were

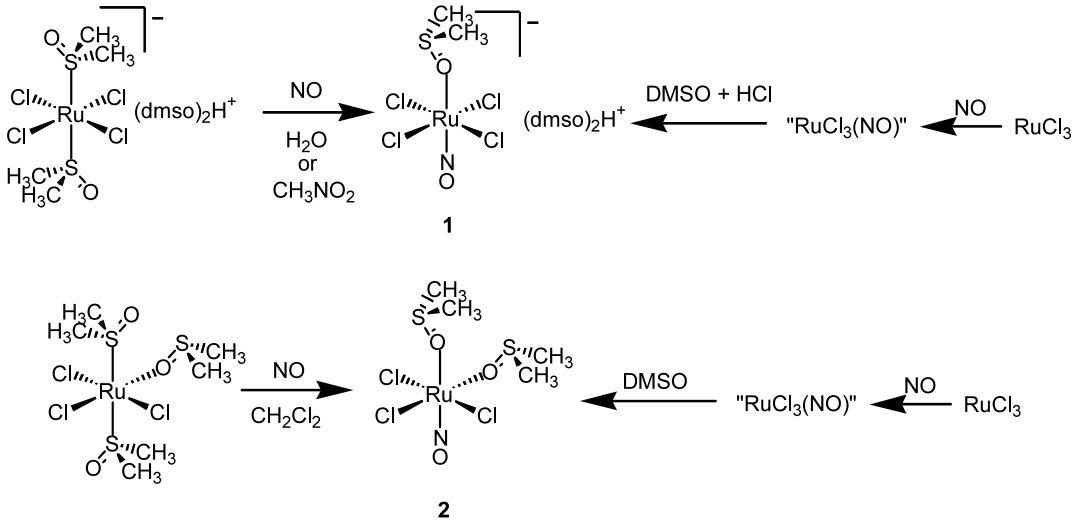

Scheme 1.

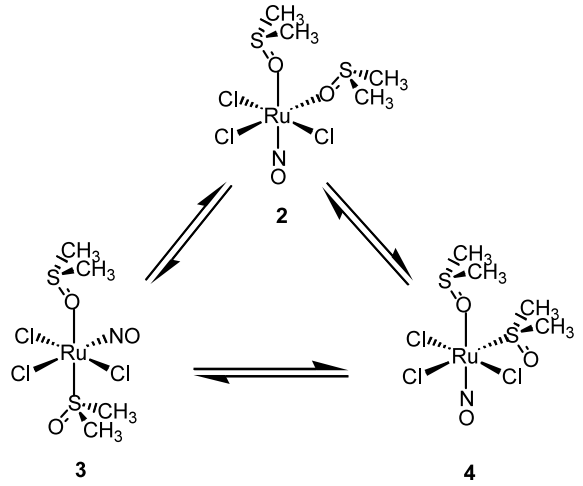

Scheme 2.

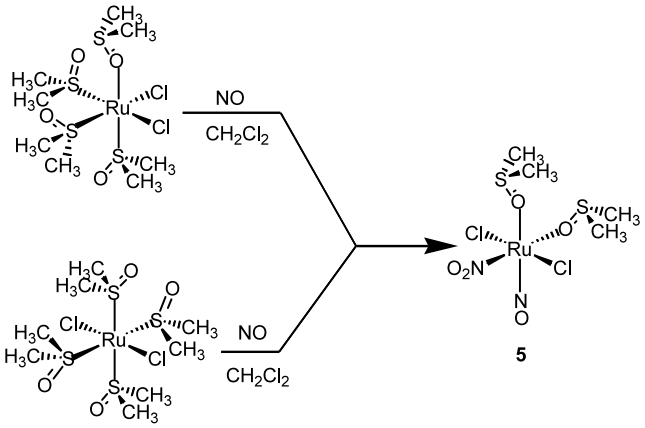

Scheme 3.

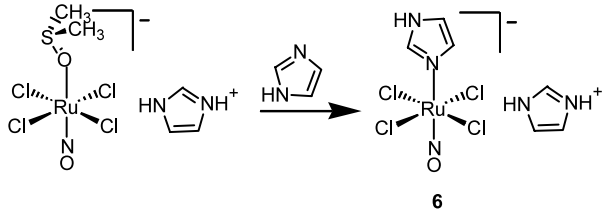

Scheme 4.

obtained on a Jasco V-550 spectrometer in quartz cells. ^{1}H-NMR and ^{13}C-NMR spectra were recorded at 400 and 100.5 MHz, respectively, on a JEOL Eclipse 400 FT instrument. ^{19}F-NMR spectra were recorded at 376.5 MHz on a Bruker Avance 400 instrument. All spectra were run at room temperature. Proton peak positions were referenced to sodium 2,2-dimethyl-2-silapentane-sulfonate (DSS) in D_2O and to the peak of residual non-deuterated solvent set at $\delta = 4.33$ ppm in CD_3NO_2. Carbon peak positions were referenced to the central peak of nitromethane set at $\delta = 62.8$ ppm. A $CDCl_3$ solution of $C_6H_5CF_3$ (set at $\delta = -67.73$ ppm) was used as external standard for fluoride spectra. Infrared spectra were recorded on a Perkin–Elmer 983G spectrometer. ESI mass spectra were obtained in methanol on a Perkin–Elmer AP1 instrument working in the positive ionization mode. Elemental analysis (C, H, N) was performed at the Dipartimento di Scienze Chimiche, Università di Trieste. Electrochemical studies were performed in DMF/0.1 M $[NBu_4][BF_4]$ as detailed previously [12,13]. Reference electrode: Ag/AgCl. Working electrode: Pt microelectrode for cyclic voltammetry and Pt basket electrode for coulometric experiments. Counterelectrode: Pt rod. Solutions were all purged with N_2 prior to electrochemical study.

2.1. *[cis,fac-RuCl$_2$(DMSO-O)$_3$(NO)][BF$_4$] (**9**)*

This complex was prepared according to Scheme 7 as follows: 0.13 g of $AgBF_4$ (0.67 mmol) was added to a solution of *mer*-$RuCl_3$(DMSO-O)$_2$(NO) (0.250 g, 0.635 mmol) in 15 ml of nitromethane and 0.15 ml of DMSO. The mixture was refluxed for 2 h and then filtered to remove AgCl. The dark-red solution was concentrated to an oil and then redissolved in 10 ml of acetone, and diethyl ether (1 ml) was added. The product precipitated slowly as a pink orange microcrystalline solid from the solution stored at 4 °C and was removed by filtration, washed with cold acetone, diethyl ether and vacuum dried. A further crop of product was obtained from the concentrated mother liquor upon addition of a small amount of diethyl ether. Yield: 0.14 g (42%). The product was recrystallized from acetone upon addition of diethyl ether. MW: 523.17 [$C_6H_{18}N_1BCl_2F_4O_4S_3Ru$]. Elemental analysis—Calc.: C, 13.7; H, 3.47; N, 2.68. Found: C, 13.8; H, 3.83; N, 2.84%. ESI-MS: *m/e* = 436.7 (Calc. for $[RuCl_2(DMSO\text{-}O)_3(NO)]^+$, 436.3). ^{1}H-NMR spectrum in D_2O (ppm): 3.09 (s, 6H, DMSO-*O*), 2.98 (s, 6H, DMSO-*O*), 2.96 (s, 6H, DMSO-*O*). ^{13}C{^{1}H}-NMR spectrum in D_2O (ppm): 34.9, 34.8, 34.7 (DMSO-*O*). Selected IR (KBr, cm^{-1}): $\nu_{N\equiv O}$, 1899 (vs); $\nu(BF_4^-)$, 1069 (vs); ν_{SO}, 911 (vs, DMSO-*O*); ν_{Ru-O}, 519, 498 (m); ν_{Ru-Cl}, 346 (m). Visible spectrum (H_2O): λ_{max}, 480 nm ($\varepsilon = 60$ dm^3 mol^{-1} cm^{-1}).

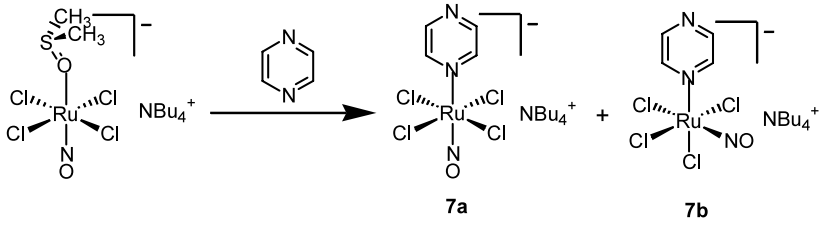

Scheme 5.

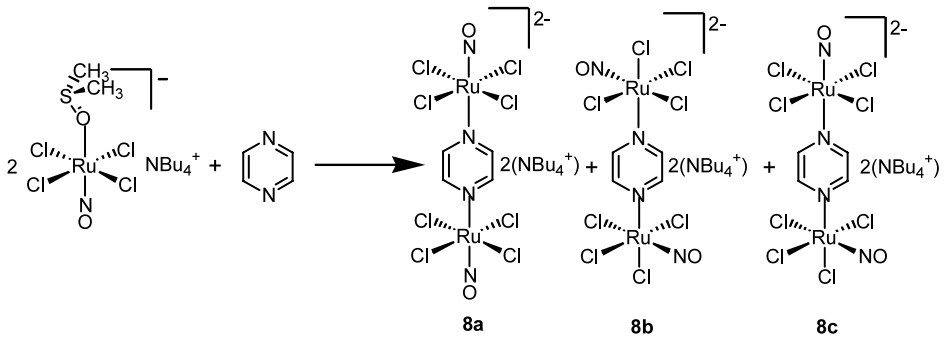

Scheme 6.

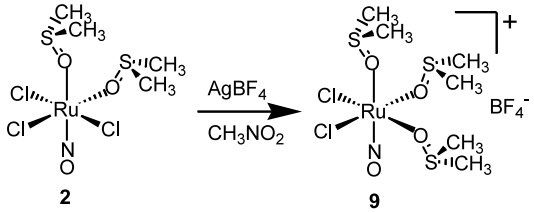

Scheme 7.

2.2. *[cis,mer-RuCl$_2$(py)$_3$(NO)][BF$_4$] (**10**)*

This complex was prepared according to Scheme 8 as follows: 51 μl of pyridine (0.63 mmol) was added to a solution of **9** (0.1 g, 0.19 mmol) in 15 ml of nitromethane. The mixture was refluxed under Ar for 1 h, during which time the color changed from light-orange to bright-red. Concentration of the solution to ca. 4 ml yielded a small amount of a dark-pink precipitate that was removed by filtration, washed with cold nitromethane and diethyl ether (this product was later established to be RuCl$_3$(py)$_2$(NO) (**12**); see below). The mother liquor was concentrated to an oil, redissolved in 5 ml of acetone, to which a few drops of diethyl ether were added. The product precipitated slowly as a light-orange solid and was removed by filtration, washed with cold acetone, diethyl ether and vacuum dried. Yield: 20 mg (20%). MW: 526.09 [$C_{15}H_{15}N_4BCl_2F_4ORu$]. Elemental analysis—Calc.: C, 34.2; H, 2.87; N, 10.65. Found: C, 33.9; H, 2.73; N, 10.45%. ESI-MS: $m/e = 440.0$ (Calc. for [RuCl$_2$(py)$_3$(NO)]$^+$, 439.3). ^{1}H-NMR spectrum in CD_3NO_2 (ppm): 8.70 (d, 4H, *o*H), 8.53 (d, 2H, *o*H), 8.23 (m, 3H, *p*H), 7.70 (m, 6H, *m*H). ^{19}F-NMR spectrum in CD_3NO_2 (ppm): −157.86 ($^{10}BF_4^-$), −157.93 ($^{11}BF_4^-$). Selected IR (KBr, cm^{-1}): $\nu_{N\equiv O}$, 1899 (vs); $\nu(BF_4^-)$, 1069 (vs); ν_{Ru-Cl}, 345, 328 (m). Visible spectrum (CH_3NO_2): λ_{max}, 484 nm ($\varepsilon = 125$ dm^3 mol^{-1} cm^{-1}).

2.3. *[cis,mer-RuCl(F)(py)$_3$(NO)][BF$_4$] (**11**)*

The above reaction was performed in refluxing chloroform (25 ml plus five drops of nitromethane to increase the solubility of the precursor **9**) for 4 h under Ar. The resulting deep-yellow solution was filtered over fine paper to remove a slight amount of precipitate (compound **12**; see below) and then concentrated to an oil and redissolved in 5 ml of methanol. A small amount of a dark-pink precipitate was removed by filtration, washed with cold methanol and diethyl ether (this product was later established to be RuCl$_3$(py)$_2$(NO) (**12**); see below). The main product precipitated slowly as a light-orange solid and was removed by filtration, washed with cold methanol, diethyl ether and vacuum dried. Yield: 15 mg (15%). MW: 509.63 [$C_{15}H_{15}N_4BClF_5ORu$]. Elemental analysis—Calc.: C, 35.3; H, 2.97; N, 10.99. Found: C, 34.7; H, 2.85; N, 10.56%. ESI-MS: $m/e = 422.8$ (Calc. for [RuCl(F)(py)$_3$(NO)]$^+$, 422.8). ^{1}H-NMR spectrum in CD_3NO_2 (ppm): 8.68 (d, 4H, *o*H), 8.50 (d, 2H, *o*H), 8.22 (m, 3H, *p*H), 7.72+7.67 (m, 6H, *m*H). ^{19}F-NMR spectrum in CD_3NO_2 (ppm): −122.41 (s, Ru–*F*), −157.86 ($^{10}BF_4^-$), −157.93 ($^{11}BF_4^-$). Selected IR (KBr, cm^{-1}): $\nu_{N\equiv O}$, 1895 (vs); $\nu(BF_4^-)$, 1069 (vs); ν_{Ru-F}, 547 (m); ν_{Ru-Cl}, 339 (m). Visible spectrum (CH_3NO_2): λ_{max}, 447 nm ($\varepsilon = 125$ dm^3 mol^{-1} cm^{-1}).

When diethyl ether was added to the methanol solution to induce precipitation and increase the reaction yield, a ca. 1:1 mixture of **10** and **11** was obtained (total yield ca. 40%).

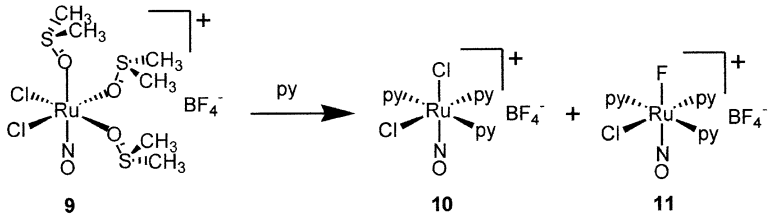

Scheme 8.

2.4. $RuCl_3(py)_2(NO)$ (**12**)

Compound **12** precipitated as a dark-pink solid from the reaction medium in the preparations of both **10** and **11**, as detailed above. Average yield: ca. 17 mg (22%). MW: 395.43 [$C_{10}H_{10}N_3Cl_3ORu$]. Elemental analysis—Calc.: C, 30.3; H, 2.55; N, 10.62. Found: C, 30.2; H, 2.54; N, 10.2. ^{1}H-NMR spectrum in CD_3NO_2 (ppm): 9.10 (d, 4H, *o*H), 8.14 (m, 2H, *p*H), 7.66 (m, 4H, *m*H). Selected IR (KBr, cm^{-1}): $\nu_{N\equiv O}$, 1850 (vs); ν_{Ru-Cl}, 351, 329 (m).

As an alternative, **12** was prepared by treatment of *mer*,*cis*-$RuCl_3(DMSO\text{-}O)_2(NO)$ (**2**) with pyridine: 104 μl of pyridine (1.26 mmol) was added to a suspension of **2** (0.1 g, 0.25 mmol) in 30 ml of chloroform. The mixture was refluxed under Ar for 4 h, during which time the color changed from light-orange to bright-red. A dark-pink precipitate was obtained upon concentration of the final solution to ca. 3 ml and addition of some diethyl ether; it was removed by filtration, washed with cold chloroform, diethyl ether and vacuum dried. Yield: 30 mg (30%).

2.5. X-ray crystallography

Diffraction data for the structures **9**–**11** were carried out on a Nonius DIP-1030H system with Mo–K_α radiation. A total of 30 frames were collected, each with an exposure time of 15–20 min, rotation angle of 6° about φ, the detector at 80 mm from the crystal. Cell refinement, indexing and scaling of the data sets were carried out using Mosflm [14] and Scala [14]. All the structures were solved by Patterson and Fourier analyses [15] and refined by the full-matrix least-squares method based on F^2 with all observed reflections [15]. All the calculations were performed using the WinGX System, Ver 1.64.02 [16].

Crystal data (**9**): $C_6H_{18}BCl_2F_4NO_4RuS_3$, $M = 523.17$, triclinic, space group $P\bar{1}$, $a = 8.681(3)$ Å, $b = 9.584(3)$ Å, $c = 12.882(4)$ Å, $\alpha = 76.02(2)^\circ$, $\beta = 76.36(2)^\circ$, $\gamma = 100.74(2)^\circ$, $V = 976.5(5)$ Å^3, $Z = 2$, $\rho_{Calc} = 1.779$ g cm^{-3}, μ(Mo–K_α) = 1.441 mm^{-1}, $F(0\,0\,0) = 520$. Final $R_1 = 0.0514$, $wR_2 = 0.1467$, $S = 1.065$ for 206 parameters and 6516 reflections, 4027 unique [$R_{int} = 0.0395$], of which 3581 with $I > 2\sigma(I)$, max positive and negative peaks in ΔF map 0.860, −0.568 e Å^{-3}.

Crystal data (**10**): $C_{15}H_{15}BCl_2F_4N_4ORu$, $M = 526.09$, orthorhombic, space group *Pbca*, $a = 11.926(4)$ Å, $b = 12.398(4)$ Å, $c = 27.530(5)$ Å, $V = 4071(2)$ Å^3, $Z = 8$, $\rho_{Calc} = 1.717$ g cm^{-3}, μ(Mo–K_α) = 1.081 mm^{-1}, $F(0\,0\,0) = 2080$. Final $R_1 = 0.0554$, $wR_2 = 0.1469$, $S = 1.062$ for 253 parameters and 8713 reflections, 4562 unique [$R_{int} = 0.0381$], of which 3086 with $I > 2\sigma(I)$, max positive and negative peaks in ΔF map 1.909 [close to Ru centre], −0.547 e Å^{-3}.

Crystal data (**11**): $C_{15}H_{15}BClF_5N_4ORu$, $M = 509.64$, orthorhombic, space group *Pbca*, $a = 11.388(3)$ Å, $b = 12.465(3)$ Å, $c = 27.274(5)$ Å, $V = 3871.6(16)$ Å^3, $Z = 8$, $\rho_{Calc} = 1.749$ g cm^{-3}, μ(Mo–K_α) = 1.007 mm^{-1}, $F(0\,0\,0) = 2016$. Final $R_1 = 0.0498$, $wR_2 = 0.1283$, $S = 1.063$ for 253 parameters and 8307 reflections, 4285 unique [$R_{int} = 0.0269$], of which 3180 with $I > 2\sigma(I)$, max positive and negative peaks in ΔF map 0.947, −0.500 e Å^{-3}.

3. Results

3.1. Recent relevant results

Until very recently [12,13,17], despite the large number of ruthenium-nitrosyls described in the literature [1,18], the examples involving sulfoxide derivatives were very few and the structural characterizations available were of low quality [19–21].

We investigated the reactivity of several Ru(II) and Ru(III)–chloride–DMSO precursors and of the antimetastatic drug NAMI-A towards NO. Treatment of $[(DMSO)_2H][trans\text{-}RuCl_4(DMSO\text{-}S)_2]$ and *mer*-$RuCl_3(DMSO)_3$ with gaseous NO yielded $[(DMSO)_2H][trans\text{-}RuCl_4(DMSO\text{-}O)(NO)]$ (**1**) and *mer*,*cis*-$RuCl_3(DMSO\text{-}O)_2(NO)$ (**2**), respectively (Scheme 1) [12]. Coordination of the strong π-acceptor NO induces an S to O linkage isomerization of the DMSO *trans* to it to avoid competition for π electrons. The same neutral nitrosyl complex **2** was obtained by us [12] and by others [17] by treatment of the $RuCl_3(NO)$ intermediate with DMSO. Similarly, treatment of $RuCl_3(NO)$ with DMSO+HCl yields compound **1**. In light-protected nitromethane solutions, complex **2** equilibrates slowly with the two isomers *mer*-$RuCl_3(DMSO\text{-}S)(DMSO\text{-}O)(NO)$ (**3**) with NO *trans* to Cl and *mer*-$RuCl_3(DMSO\text{-}S)(DMSO\text{-}O)(NO)$ (**4**) with NO *trans* to DMSO-O (Scheme 2); the equilibrium mixture consists of ca. 64% **2**, 3% **3** and 33% **4**.

Treatment of either Ru(II)–DMSO precursor, *trans*-$RuCl_2(DMSO\text{-}S)_4$ or *cis*-$RuCl_2(DMSO)_4$, with gaseous NO in CH_2Cl_2 solution yielded the nitrosyl-nitro derivative *trans*,*cis*,*cis*-$RuCl_2(DMSO\text{-}O)_2(NO)(NO_2)$ (**5**) (Scheme 3), which can be thought of as deriving from **2** upon replacement of the chloride *trans* to DMSO-O with the nitro group [12].

Finally, $[(Im)_2H][trans\text{-}RuCl_4(Im)(NO)]$ (**6**) was prepared by treatment of $[ImH][trans\text{-}RuCl_4(DMSO\text{-}O)(NO)]$ with an excess of imidazole in refluxing acetone (Scheme 4) [12]. Similarly, by treatment of the tetrabutylammonium salt of **1** with pyrazine we also prepared some mono- and dinuclear ruthenium nitrosyls bearing either terminal ($[NBu_4][trans\text{-}RuCl_4(pyz)(NO)]$ (**7a**) and $[NBu_4][cis\text{-}RuCl_4(pyz)(NO)]$ (**7b**); Scheme 5) or bridging pyrazine ($[NBu_4]_2[\{trans/cis\text{-}RuCl_4(NO)\}_2(\mu\text{-}pyz)]$ (*trans*,*trans*-**8a**, *cis*,*cis*-**8b**, *trans*,*cis*-**8c**); Scheme 6) [13].

The spectroscopic features for each of the above complexes are consistent with the $\{Ru(NO)\}^6$ formulation, i.e. a diamagnetic Ru(II) nucleus bound to NO^+. Compounds **1**, **2**, **5**, **6**, **7a** and **7b** were also characterized by X-ray crystallography [12,13]; they all show a linear nitrosyl

group, with short Ru–NO bond distances consistent with a strong $d_\pi \rightarrow \pi^*$ NO back bonding. An unusual inertness of O-bonded DMSO was observed in compound **1**.

Complexes **1**, **2**, **3**, **5** and **6** are all redox active in DMF solutions showing irreversible reductions whose peak potentials depend on the other ligands attached to the Ru metal center. There was no improvement in the reversibility of the reduction process for all DMSO-containing compounds at low temperature, down to 223 K, and/or by increasing the scan rate to 20 V s^{-1}. The site of reduction is the NO^+ moiety. The reduced complexes are not stable and rapidly release a Cl^- ligand (or NO_2^- in the case of **5**) followed by the $NO^\bullet$ radical. The chemical reactions following electron transfer are all fast; rate constants $> 100\ s^{-1}$ at 293 K were inferred from the electrochemical studies. The Ru product species are not redox active within the DMF window.

3.2. New results

We find now that treatment of *mer*,*cis*-$RuCl_3$(DMSO-O)$_2$(NO) (**2**) with an equivalent amount of $AgBF_4$ in refluxing nitromethane and DMSO leads to the isolation of the cationic species [*cis*,*fac*-$RuCl_2$(DMSO-O)$_3$(NO)][BF_4] (**9**), in which all three DMSO ligands are bound through oxygen in a facial geometry (Scheme 7). The NO stretching frequency in **9** is ca. 20 cm^{-1} higher than in its precursor **2**, owing to the expected decrease of the π back bonding contribution in the Ru–NO bond upon going from a neutral to a cationic complex. Consistent with the $\{Ru(NO)\}^6$ formulation, complex **9** is diamagnetic; three equally intense singlet resonances are found in the DMSO-O region of its ^{1}H-NMR spectrum: the sharpest one (δ=3.09) belongs to the equivalent methyl groups of the DMSO-O *trans* to NO, while the other two (δ = 2.98 and 2.96) pertain to the diastereotopic methyl groups of the two equivalent DMSO's *trans* to Cl and are slightly broadened by the long-range coupling. These two resonances are connected in the H-H COSY spectrum. It should be noted that a similar set of NMR signals is expected also for the [*cis*,*mer*-$RuCl_2$(DMSO-O)$_3$(NO)]$^+$ isomer; the geometry of **9** was established unambiguously only by determination of its X-ray structure (see below). As found for the other complexes of this series studied previously [12], also compound **9** is quite inert; for example, in a light-protected D_2O solution of **9**, only ca. 25% of the coordinated DMSO-O is hydrolyzed over a period of 8 days at room temperature.

Treatment of **9** in refluxing organic solvents with *N*-heterocyclic ligands L such as pyridine (py) led to the replacement of all three DMSO moieties and to the isolation of [$RuCl_2$(py)$_3$(NO)][BF_4] (**10**) (Scheme 8). Pure **10**, even though in relatively low yield, was obtained when the reaction between **9** and pyridine was performed in refluxing nitromethane followed by crystallization from acetone. TLC and ^{1}H-NMR analyses showed that the mother liquor contained, beside residual **10**, a number of unidentified products with coordinated py (including **11**; see below). The geometry of compound **10**, whose NO stretching frequency is substantially unchanged compared to **9**, could not be established by NMR spectroscopy only, since all three possible isomers, [*fac*-$RuCl_2$(py)$_3$(NO)]$^+$, [*trans*,*mer*-$RuCl_2$(py)$_3$(NO)]$^+$ and [*cis*,*mer*-$RuCl_2$(py)$_3$(NO)]$^+$, are expected to have similar patterns for the py resonances (two sets of signals in a 2:1 intensity ratio). X-ray analysis (see below) established that the isolated complex **10** has the *cis*,*mer* geometry, implying that replacement of DMSO-O by pyridine is accompanied by isomerization that brings NO *trans* to Cl. Formation of a *fac*-[$RuCl_2$(Im)$_3$(NO)]$^+$ complex (Im = imidazole) was postulated to occur (on the basis of IR data) upon treatment of $RuCl_3$(NO)(H_2O)$_2$ with three equivalents of imidazole in aqueous solution [4b]; this complex however is apparently fluxional and an averaged set of NMR signals for the three imidazole ligands was found in D_2O. No sign of fluxional behavior on the ^{1}H-NMR time scale was found in the case of **10**.

When the reaction was performed in refluxing chloroform, followed by crystallization from methanol, the isolated raw product was composed, according to ^{1}H-NMR analysis, of comparable amounts of **10** and of another compound, **11**, characterized by a spectrum very similar to that of **10**. Crystals of pure **11** were obtained by slow crystallization of the raw product from a dilute methanol solution to which diethyl ether was added. X-ray analysis, supported by ESI-MS and ^{19}F-NMR data, established that compound **11** derives from **10** upon substitution of the Cl *trans* to NO by F and can be thus formulated as [*cis*,*mer*-$RuCl$(F)(py)$_3$(NO)][BF_4] (Scheme 8). The only source of fluorine in this reaction is the BF_4 anion; several precedents for the formation of fluoro complexes from BF_4^- can be found in the literature [22]. Interestingly, no halide scrambling was observed to occur in the preparation of the cationic precursor **9**, which is performed under more forcing conditions.

During the preparation of **10**, regardless of the reaction conditions, a relatively small amount of yet another nitrosyl product, **12**, precipitates from the solution. The ^{1}H-NMR spectrum of **12** in CD_3NO_2 solution, in which the complex is slightly soluble, shows no resonances for coordinated DMSO and only one set of py signals. According to elemental analysis, compound **12** can be formulated as the neutral species $RuCl_3$(py)$_2$(NO), which must derive from **9** upon replacement of the three sulfoxides with two pyridine molecules and one chloride deriving from **9** itself. In addition, complex **12** was also obtained as main product upon treatment of the neutral precursor **2** with py in refluxing chloroform, thus allowing the possibility of coordinated fluoride to be eliminated. Two geometries, *fac*-$RuCl_3$(py)$_2$(NO) and *mer*,*trans*-$RuCl_3$(py)$_2$(NO), are consistent with the observed NMR pattern of **12** as they have equivalent pyridine ligands, but could not be distinguished. In both geometries NO is *trans* to a chloride. The NO stretching frequency in **12** is ca. 30 cm^{-1} lower than in the precursor **2**, in which NO is *trans* to a DMSO-O ligand. Shepherd and coworkers [4b], on the basis of NMR data, reported that treatment

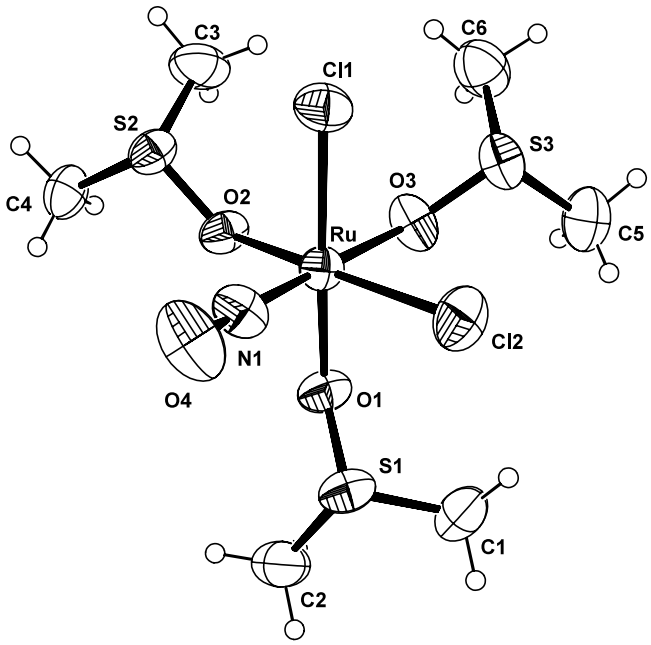

Fig. 1. Molecular structure and atom numbering scheme of the cation of [*cis*,*fac*-$RuCl_2(DMSO\text{-}O)_3(NO)][BF_4]$ (**9**) (ortep drawing, 40% probability level). Selected bond lengths (Å) and angles (°): Ru–N(1), 1.727(4); Ru–Cl(1), 2.347(1); Ru–Cl(2), 2.335(1); N(1)–O(4), 1.139(6); Ru–O(1), 2.074(3); Ru–O(2), 2.063(3); Ru–O(3), 2.028(3); N(1)–Ru–O(3), 178.3(2); O(1)–Ru–Cl(1), 170.15(9); O(2)–Ru–Cl(2), 169.3(1); Ru–N(1)–O(4), 173.5(4); Ru–O(1)–S(1), 120.9(2); Ru–O(2)–S(2), 123.9(2); Ru–O(3)–S(3), 122.7(2).

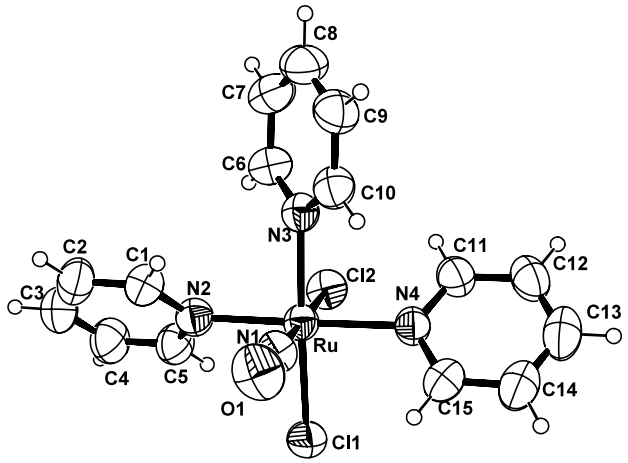

Fig. 2. Molecular structure (ortep drawing, 40% probability level) of the cation of [*cis*,*mer*-$RuCl_2(py)_3(NO)][BF_4]$ (**10**). The atom numbering scheme applies also to **11**, substituting Cl(2) with a fluorine atom. Selected bond lengths (Å) and angles (°) (for **11**, data in italics): Ru–N(1), 1.749(4) (*1.749(3)*); Ru–N(2), 2.106(4) (*2.096(4)*); Ru–N(3), 2.116(4) (*2.095(4)*); Ru–N(4), 2.115(4) (*2.106(4)*); Ru–Cl(2), 2.325(1) (*1.984(2)*); Ru–Cl(1), 2.368(1) (*2.367(1)*); N(1)–O(1), 1.131(5) (*1.133(4)*); O(1)–N(1)–Ru, 177.6(4) (*176.9(4)*).

of $RuCl_3(NO)(H_2O)_2$ with two equivalents of imidazole in aqueous solution leads to the formation of a mixture of both *fac*-$RuCl_3(Im)_2(NO)$ and *mer*,*trans*-$RuCl_3(Im)_2(NO)$ isomers.

3.3. X-ray crystallography

The molecular structures of complexes **9** and **10** are shown in Figs. 1 and 2, respectively (the structure of **11**, which is isomorphous to **10**, is not reported since it can be obtained from that of **10** by replacement of Cl(2) with F). Selected bond lengths and angles are reported in the corresponding captions. In all the complexes, the metal displays a distorted octahedral geometry with a linear nitrosyl group which is *trans* to an O-bonded DMSO in **9**, to a chloride in **10** and to a fluoride in **11**. The X-ray structures of **9**–**11** provided evidence that: (i) the three DMSO-O ligands in **9** have a facial geometry and (ii) their replacement by the pyridines is accompanied by a *fac* to *mer* isomerization. A common feature in **9**–**11**, already observed in previous nitrosyls of this series, is the displacement of the metal from the mean "basal" plane towards the NO group. In fact, in **9** ruthenium is displaced from the Cl(1)/Cl(2)/O(1)/O(2) plane by about 0.17 Å, while the corresponding values in **10** and **11** are lower (0.07 and 0.11 Å, respectively).

Compound **9** represents the second example of a ruthenium complex bearing three O-bonded DMSO ligands; the previous example, the dicationic species [*fac*-$Ru(DMSO\text{-}O)_3(DMSO\text{-}S)_3]^{2+}$, was reported more than 20 years ago [23]. The Ru–Cl bond distances (Ru–Cl(1) = 2.347(1) Å, Ru–Cl(2) = 2.335(1) Å) fall in the usual range reported in the literature for Ru(II) complexes. On the other hand, a slight shortening is observed for the Ru–O bond length *trans* to the nitrosyl group (2.028(3) Å) when compared with the other values (2.063(3) and 2.074(3) Å). This difference is attributed to the well-documented *trans*-shortening effect exerted by NO when coordinated *trans* to a σ-donor ligand [18b,24]. We found similar short Ru–O bond lengths in the X-ray structures of $[(DMSO)_2H][trans\text{-}RuCl_4(DMSO\text{-}O)(NO)]$ (**1**), *mer*,*cis*-$RuCl_3(DMSO\text{-}O)_2(NO)$ (**2**) and *trans*,*cis*,*cis*-$RuCl_2(DMSO\text{-}O)_2(NO)(NO_2)$ (**5**) [12]. Following the suggestions of Geremia and Calligaris [25], the conformation of all the DMSO ligands in **9** can be classified as *trans*-*trans* (Ru–O–S–C torsion angles between −107° and −153°). This arrangement, likely dictated by inter-ligand steric interactions, is markedly preferred by this ligand in the solid state [26].

The Ru–NO bond length of 1.727(4) Å in **9** appears sensibly shorter then those detected in the pyridine derivatives **10** and **11** (1.749(4) Å). On the other hand, in all the structures, the N–O distances are comparable within their e.s.d.s (range: 1.131(5)–1.139(6) Å). These data are in agreement with spectroscopic results that show no significant difference in the NO stretching frequency between **9** and **10** (or **11**).

In **10** and **11**, the Ru–N(py) bond lengths fall in a range from 2.095(4) to 2.116(4) Å, with the pyridine ligands oriented in such a way to bisect the coordination bond angles in *cis*-position. Both the structures have comparable Ru–Cl(1)

bond distances, but the Ru–Cl(2) *trans* to NO in **10** is shorter (2.325(1) Å). The Ru–F bond distance found in **11**, which agrees nicely with the typical Ru–F distances found in the literature [27], corresponds to the value calculated by subtracting the difference between the covalent radii of Cl and F (0.35 Å) from the Ru–Cl distance determined in **10**. This suggests that both fluoride and chloride manifest push-pull interactions of comparable magnitude, as can be deduced also from the strictly similar Ru–NO and N–O bond distances (and NO stretching frequencies) in the two isomorphous halide derivatives.

3.4. Electrochemical studies

DMF was chosen as the solvent for the electrochemical studies, as all the complexes were soluble in this solvent hence common solvent could be employed. Furthermore, experiments confirmed that DMF did not substitute into the complexes in their starting form. Owing to the potential biological implications of these nitrosyls, ultimately we would want to consider their redox chemistry in an aqueous medium. However, water does not permit study at low temperature and is not a good epr solvent particularly for spectroelectrochemical investigations.

3.4.1. [*cis*,*fac*-$RuCl_2(DMSO\text{-}O)_3(NO)][BF_4]$ (**9**)

As for other ruthenium–DMSO nitrosyls studied previously, [*cis*,*fac*-$RuCl_2(DMSO\text{-}O)_3(NO)][BF_4]$ (**9**) exhibits an irreversible one-electron (as determined by coulometry) reduction. The peak potential of the reduction is measured at −0.26 V at 100 mV s^{-1} at room temperature as shown in Fig. 3.

Decreasing the temperature to 233 K and increasing the scan rate to 1 V s^{-1} did not result in any sign of reversibility. Thus, once again the electron transfer reaction is followed by a rapid chemical reaction. Bulk electrolysis of the solution by one molar equivalent of electrons at −0.42 V is accompanied by collapse of the NO band at 1878.2 cm^{-1}.

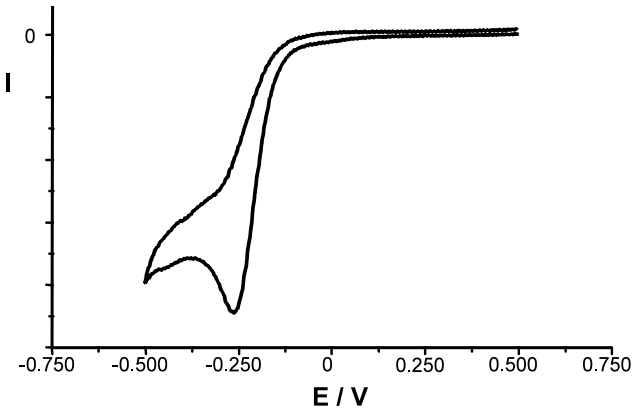

Fig. 3. Cyclic voltammetric response for [*cis*,*fac*-$RuCl_2(DMSO\text{-}O)_3(NO)][BF_4]$ (**9**) in DMF/0.1 M $[NBu_4][BF_4]$ at 298 K, scan rate 0.1 V s^{-1}.

The resulting solution shows no electrochemical responses from +1.5 to −1.5 V, i.e. the product species formed following reduction is not electrochemically active and no chloride ligands are released as a result of the reduction. We believe that once again, and in common with the previous studies, the NO^+ ligand is being reduced and the following mechanism is occurring (Eq. (1)):

$$\text{Ru(II)—NO}^+ + e^- \rightarrow \text{Ru(II)—NO}^\bullet \rightarrow \text{Ru(II)—DMF} + \text{NO} \quad (1)$$

Compared to previously studied anionic and neutral nitrosyls of this series, replacement of a further chloride ligand by a DMSO ligand has resulted in the positive shift of the reduction peak (Table 1).

This is to be expected as replacement of the π-donor chloride ligand by the σ-donor DMSO-O ligand will result in decreased electron density at the Ru(II) center which will, in turn, result in decreased back donation from the Ru(II) to the π*-antibonding orbital of the NO^+. Thus, it will be easier to reduce the NO^+ ligand, hence the observed shift of the reduction potential to less negative potentials as chloride ligands are sequentially replaced by DMSO ligands.

3.4.2. [*cis*,*mer*-$RuCl_2(py)_3(NO)][BF_4]$ (**10**)

Replacement of the DMSO-O ligands in **9** by pyridine to give [*cis*,*mer*-$RuCl_2(py)_3(NO)][BF_4]$ (**10**) results in the cyclic voltammetric trace shown in Fig. 4. The one-electron reduction process now becomes reversible, with a half wave potential at −0.11 V. A further irreversible reduction is observed at −1.00 V. Since pyridine can be regarded as a weak π-accepting ligand, replacement of DMSO by py should and does result in a positive potential shift of the NO^+-based reduction. Thus, we assign the reversible reduction to the

Table 1
Reduction peak potentials of $[RuCl_{5-x}(DMSO)_x(NO)]^{(x-2)}$ complexes ($x = 1$, 2, 3 in DMF/0.1 M NBu_4BF_4 at 298 K, scan rate 0.1 V s^{-1}), compared to those of other Ru-nitrosyls

Compound	NO^+-based reduction potential[a]	Reference
$[Ru(bpy)_2(NO)(CH_3CN)]^{3+}$	0.57	[28]
$[Ru(bpy)_2(NO)(py)]^{3+}$	0.54	[28]
$[Ru(bpy)_2(NO)(NH_3)]^{3+}$	0.37	[28]
$[Ru(bpy)_2(NO)(NO_2)]^{2+}$	0.34	[28]
$[Ru(bpy)_2(NO)(Cl)]^{2+}$	0.20	[28]
$[Ru(bpy)_2(NO)(N_3)]^{2+}$	0.18	[28]
$[Ru(bpy)(trpy)(NO)]^{3+}$	0.46	[28]
$[Ru(NO)(NH_3)_5]^{3+}$	−0.35	[28,29]
$[Ru(NO)(NH_3)_4(py)]^{3+}$	−0.25	[29]
$[Ru(NO)(NH_3)_4(L\text{-hist})]^{3+}$	−0.39	[29]
$[Ru(NO)(NH_3)_4(P(OMe)_3)]^{3+}$	−0.12	[29]
$[RuCl(NO)(cyclam)]^{2+}$	−0.27	[3a]
[Ru(trpy)(azopyridine)(NO)]$^{3+}$	0.37	[30]
trans-$[RuCl_4(DMSO\text{-}O)(NO)]^-$	−1.25 (irreversible)	[12]
mer,*cis*-$RuCl_3(DMSO\text{-}O)_2(NO)$	−0.59 (irreversible)	[12]
cis,*fac*-$[RuCl_2(DMSO\text{-}O)_3(NO)]^+$	−0.26 (irreversible)	This work
cis,*mer*-$[RuCl_2(py)_3(NO)]^+$	−0.11	This work

[a] Reversible reduction potential vs s.c.e. unless stated otherwise.

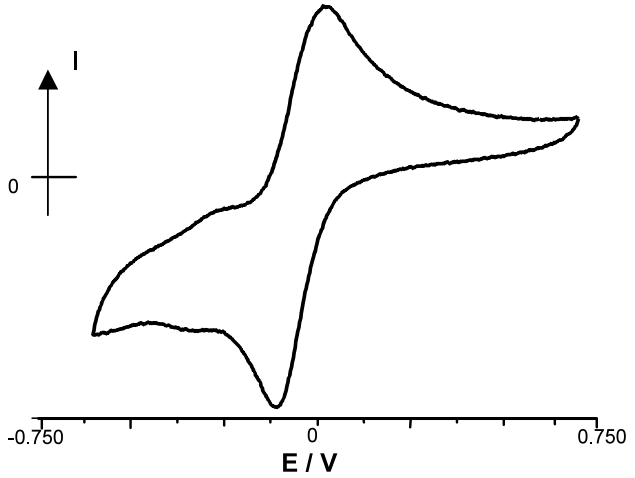

Fig. 4. Cyclic voltammetric response for [*cis*,*mer*-$RuCl_2(py)_3(NO)$] (**10**) in DMF/0.1 M [NBu_4][BF_4] at 298 K, scan rate 0.1 V s^{-1}. The scan reported is in fact the second scan although the first scan is very similar to it. The initial potential (E_i) was +0.7 V and the switching potential −0.6 V; thus, scan direction was negative initially.

following process (Eq. (2)):

$$[cis, mer\text{-}Ru(II)Cl_2(py)_3(NO^+)]^+ + e^- \leftrightarrow [cis, mer\text{-}Ru(II)Cl_2(py)_3(NO^\bullet)] \quad (2)$$

A similar behavior was observed by Callahan and Meyer [28] on $[Ru(bpy)_2(NO)Cl]^{2+}$, with a reversible one-electron reduction at +0.20 V and an irreversible reduction at −0.60 V. Bipyridine is a better π-accepting ligand than py and there is only one chloride ligand in that case and therefore the bpy analogue is expected to reduce at more positive potentials than **10**, as observed experimentally. The irreversible process is assigned to the one-electron reduction of Ru–$NO^\bullet$ to Ru–NO^- which is rapidly followed by a chemical reaction. A second and smaller process with a half wave potential at −0.29 V was observed. This minor reversible process was attributed to the presence of a trace amount of the chlorofluoro compound **11** (confirmed by NMR analysis of the sample). This attribution agrees well with Lever's [31] ligand additivity data: a shift of the observed redox couple by 0.16 V in a negative direction is anticipated by exchanging of one chloride (−0.24 V) for one fluoride ligand (−0.42 V), just as is observed. In addition, changing chloride for fluoride should still give a reversible peak.

The chemical reversibility of the main process allowed us to characterize the monoreduced species for the first time. Coulometry of the solution at room temperature revealed that the reduction process involves one electron and that the reduced species [*cis*,*mer*-$RuCl_2(NO)py_3$] is not particularly stable at 297 K. Therefore, the in situ spectroelectrochemical experiments (UV–vis spectra recorded as [*cis*,*mer*-$RuCl_2(NO)py_3$][BF_4] was reduced to the neutral species at −0.475 V) were conducted at 233 K in order to slow down any following chemical reactions. The spectrum of [*cis*,*mer*-$RuCl_2(py)_3(NO)$][BF_4] is essentially featureless at the dilute concentration used in this experiment; on reduction to [*cis*,*mer*-$RuCl_2(py)_3(NO)$] the growth of an intense band at ca. 320 nm and of a broad lower intensity band centered on 410 nm was observed. Similar transitions were observed by Callahan and Meyer [28] for the related bpy complex. A clean isosbestic point was observed at 270 nm, which implies a clean conversion process. In addition, the spectrum reverts to that of the starting material on reversal of the electrogeneration potential to +0.1 V. We also attempted to monitor the electron transfer reaction using IR spectroelectrochemically. The NO stretching band at 1897 cm^{-1} in the starting compound [*cis*,*mer*-$RuCl_2(NO)py_3]^+$ collapsed on reduction and grew back again on re-oxidation. However, no new growing bands which could be assigned to ligated NO radical could be identified. The NO band would be expected to shift by ca. 300 cm^{-1} (i.e. move to around 1600 cm^{-1}) on reduction [28]. Unfortunately, this region of the IR spectrum is masked by an intense absorption due to the solvent | electrolyte system. Attempts to vary the solvent and electrolyte to permit study in the relevant region were not successful.

Finally, an in situ epr study of the one-electron reduced species was performed. The monoreduced neutral species was generated at −0.475 V inside the epr cavity at 233 K. There was no observable signal at 233 K; however, on cooling the cell to 100 K a rhombic signal with the following g and a values was observed: $g_1 = 2.022$, $g_2 = 1.995$, $g_3 = 1.894$, $a_1(N) = 19.8$ G, $a_2(N) = 28.0$ G, $a_3(N) = 16.5$ G (Fig. 5). The g and a values were initially measured from the experimental spectrum and then confirmed by simulation. This signal has been interpreted as coupling of the unpaired electron to one N nucleus (the N couplings were measured on an expanded epr spectrum) and no other couplings to Ru could be identified.

These values correspond very well to those of the bpy analogue which also had no resolvable signal at room temperature but showed a frozen glass spectrum with $g_1 = 2.035$, $g_2 = 1.995$, $g_3 = 1.883$, $a_1(N) = 17$ G, $a_2(N) = 32.1$ G and

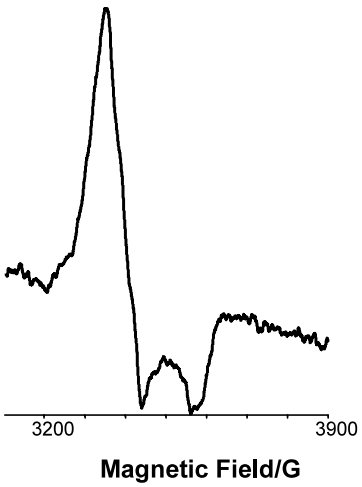

Fig. 5. Epr signal of [*cis*,*mer*-$RuCl_2(py)_3(NO)$] (**10**) at 100 K in DMF.

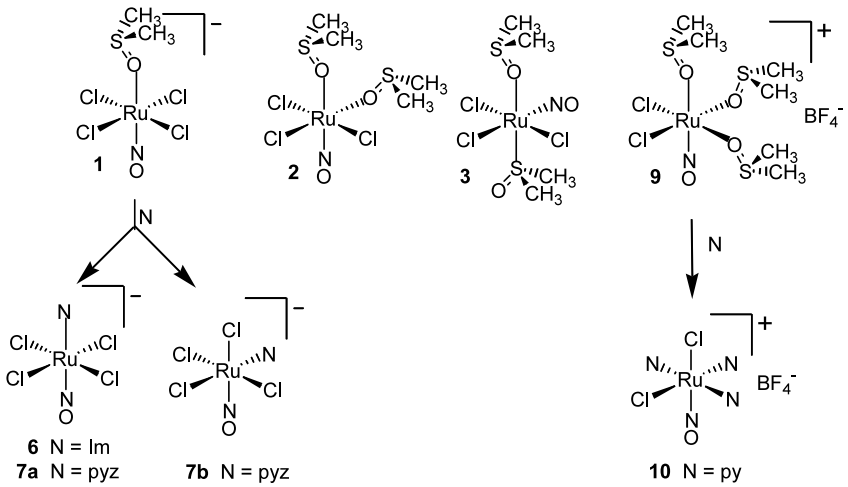

Scheme 9.

$a_3(N) = 15$ G [32]. Thus, in agreement with the explanations already given for the previous compounds of this series, all the data fit well for the reversible reduction of NO^+ on $[cis,mer\text{-}RuCl_2(py)_3(NO)]^+$ with good strong evidence of the reduced NO^+ fragment.

4. Conclusions

The possibility that the mechanism of action of the antimetastases Ru(III) compound NAMI-A, and of related Ru–DMSO species, might be due to their interference with NO metabolism in vivo prompted this investigation. Thus, we prepared and characterized a series of new Ru–DMSO nitrosyls of general formula $[RuCl_{5-x}(DMSO)_x(NO)]^{(x-2)}$ ($x = 1$–3; Scheme 9). In all cases, upon coordination of the strong π-acceptor NO to Ru, the preferred binding mode for DMSO switches from S to O. The reactivity of some Ru–DMSO nitrosyls towards heterocyclic N-ligands, leading to compounds such as $[(Im)_2H][trans\text{-}RuCl_4(Im)(NO)]$ (Im = imidazole, **6**) and $[cis,mer\text{-}RuCl_2(py)_3(NO)][BF_4]$ (py = pyridine, **10**), was also investigated (Scheme 9). The spectroscopic and X-ray structural features for all these complexes are consistent with the $\{Ru(NO)\}^6$ formulation, that is a diamagnetic Ru(II) nucleus bound to NO^+. Electrochemical measurements on the Ru–NO complexes showed that they are all redox active in DMF solutions and the site of reduction is the NO^+ moiety. With the exception of **10**, the reduced complexes are not stable and rapidly release the $NO^\bullet$ radical. The rate of NO dissociation is too fast for all compounds looked at to be measured electrochemically. Thus, the influence of the other ligands on the rate of NO dissociation could not be studied for these particular species. We also found that reducing the number of bound chloride ligands shifts the reduction potential to more positive values bringing it into a reasonable range for biological reductors.

Thus, we realized that the new ruthenium nitrosyls, besides being good models for products that may be formed in vivo from the Ru–DMSO compounds, might have themselves some pharmacological interest as potential NO-releasing agents upon in vivo reduction. Even though, for the moment, most of the chemical investigations were performed in aprotic media, ultimately we want to consider the redox chemistry in an aqueous medium. All the charged species (with the exception of **10**) are well soluble in water, where, according to preliminary ^{1}H-NMR investigations, they are quite stable also at physiological pH 7.4. In view of the possibility, evidenced by our electrochemical results, that the new nitrosyls might release NO upon reduction in vivo (and thus become cytotoxic), experiments aimed to assess their chemical behavior in aqueous solution in the presence of biological reducing agents (e.g. ascorbic acid, cysteine) will be performed, as already done for NAMI-A [6,7b]. Tests aimed to evaluate the potential cytotoxicity in vitro and anticancer activity in vivo of the new nitrosyls are currently in progress.

5. Supplementary material

Crystallographic data (excluding structure factors) reported in this paper have been deposited with the Cambridge Crystallographic Data Center, CCDC nos. 194594–194596. Copies of the data can be obtained free of charge on application to The Director, CCDC, 12 Union Road, Cambridge CB2 1EZ, UK (Fax: +44-1223-336033; e-mail: deposit@ccdc.cam.ac.uk or www: http://www.ccdc.cam.ac.uk).

Acknowledgements

We acknowledge financial support by Italian CNR (grant Agenzia 2000 C00D1EC_001) and by the Fondazione Callerio (Trieste). This work is a contribution from the Edinburgh Protein Interaction Centre (EPIC) funded by the Wellcome

Trust. Johnson Matthey is gratefully acknowledged for a generous loan of hydrated $RuCl_3$.

References

[1] (a) G.B. Richter-Addo, P. Legzdins, Metal Nitrosyls, Oxford University Press, New York, 1992;
(b) T.W. Hayton, P. Legzdins, W.B. Sharp, Chem. Rev. 102 (2002) 935.
[2] (a) S.P. Fricker, Platinum Met. Rev. 39 (1995) 150;
(b) M.T. Wilson, E. Slade, S.P. Fricker, B.A. Murrer, N.A. Powell, G.R. Henderson, Chem. Commun. (1997) 47;
(c) Y. Chen, R.E. Shepherd, J. Inorg. Biochem. 68 (1997) 183;
(d) Y. Chen, F.-T. Lin, R.E. Shepherd, Inorg. Chem. 38 (1999) 973;
(e) C.J. Marmion, T. Murphy, J.R. Docherty, K.B. Nolan, Chem. Commun. (2000) 1153;
(f) C.J. Marmion, T. Murphy, K.B. Nolan, Chem. Commun. (2001) 1870.
[3] (a) D.R. Lang, J.A. Davis, L.G.F. Lopes, A.A. Ferro, L.C.G. Vasconcellos, D.W. Franco, E. Tfouni, A. Wieraszko, M.J. Clarke, Inorg. Chem. 39 (2000) 2294;
(b) L.G.F. Lopes, A. Wieraszko, Y. El-Sherif, M.J. Clarke, Inorg. Chim. Acta 312 (2001) 15.
[4] (a) J.M. Slocik, R.E. Shepherd, Inorg. Chim. Acta 311 (2000) 80;
(b) J.M. Slocik, M.S. Ward, K.V. Somayajula, R.E. Shepherd, Transition Met. Chem. 26 (2001) 351.
[5] B.L. Wescott, J.H. Enemark, in: E.I. Solomon, A.B.P. Lever (Eds.), Inorganic Electronic Structure and Spectroscopy: Applications and Case Studies, vol. II, Wiley, New York, 1999, pp. 403–450.
[6] G. Sava, E. Alessio, A. Bergamo, G. Mestroni, in: M.J. Clarke, P.J. Sadler (Eds.), Topics in Biological Inorganic Chemistry: Metallopharmaceuticals, vol. 1, Springer, Berlin, 1999, pp. 143–169.
[7] (a) G. Sava, R. Gagliardi, A. Bergamo, E. Alessio, G. Mestroni, Anticancer Res. 19 (1999) 969;
(b) G. Sava, A. Bergamo, S. Zorzet, B. Gava, C. Casarsa, M. Cocchietto, A. Furlani, V. Scarcia, B. Serli, E. Iengo, E. Alessio, G. Mestroni, Eur. J. Cancer 38 (2002) 427.
[8] S. Zorzet, A. Bergamo, M. Cocchietto, A. Sorc, B. Gava, E. Alessio, E. Iengo, G. Sava, J. Pharmacol. Exp. Ther. 295 (2000) 927.
[9] (a) F. Murad, Angew. Chem. Int. Ed. 38 (1999) 1856;
(b) R.F. Furchgott, Angew. Chem. Int. Ed. 38 (1999) 1871;
(c) I.J. Ignarro, Angew. Chem. Int. Ed. 38 (1999) 1882.
[10] M. Ziche, L. Morbidelli, R. Choudhri, H.-T. Zhang, S. Donnini, H.J. Granger, R. Bicknell, J. Clin. Invest. 99 (1997) 2625.
[11] (a) S. Pfeiffer, B. Mayer, B. Hemmens, Angew. Chem. Int. Ed. 38 (1999) 1714;
(b) A.R. Butler, I.L. Megson, Chem. Rev. 102 (2002) 1155;
(c) J.K.S. Møller, L.H. Skibsted, Chem. Rev. 102 (2002) 1167.
[12] B. Serli, E. Zangrando, E. Iengo, G. Mestroni, L. Yellowlees, E. Alessio, Inorg. Chem. 41 (2002) 4033.
[13] B. Serli, E. Zangrando, E. Iengo, E. Alessio, Inorg. Chim. Acta 339 (2002) 265.
[14] Collaborative Computational Project, Number 4, Acta Crystallogr. D 50 (1994) 760.
[15] G.M. Sheldrick, SHELX-97, Programs for Structure analysis, University of Gøttingen, 1998.
[16] L.J. Farrugia, J. Appl. Crystallogr. 32 (1999) 837.
[17] Q.A. Paula, A.A. Batista, E.E. Castellano, J. Ellena, J. Inorg. Biochem. 90 (2002) 144.
[18] (a) R. Zarhoule, G. Duc, J. Deloume, Inorg. Chim. Acta 160 (1989) 59;
(b) B.J. Coe, T.J. Meyer, P.S. White, Inorg. Chem. 34 (1995) 593;
(c) D. Ooyama, N. Nagao, H. Nagao, Y. Miura, A. Hasegawa, K. Ando, F.S. Howell, M. Mukaida, K. Tanaka, Inorg. Chem. 34 (1995) 6;
(d) K.M. Kadish, V.A. Adamian, E. Van Caemelbecke, Z. Tan, P. Tagliatesta, P. Bianco, T. Boschi, G. Yi, M.A. Khan, G.B. Richter-Addo, Inorg. Chem. 35 (1996) 1343;
(e) D.S. Bohle, C. Hung, A.K. Powell, B.D. Smith, S. Wocaldo, Inorg. Chem. 36 (1997) 1992;
(f) S.S.S. Borges, C.U. Davanzo, E.E. Castellano, J.-Z. Schpector, S.C. Silva, D.W. Franco, Inorg. Chem. 37 (1998) 2670;
(g) M.G. Gomes, C.U. Davanzo, S.C. Silva, L.G. Lopes, P.S. Santos, D.W. Franco, J. Chem. Soc. Dalton Trans. (1998) 601;
(h) H. Nagao, K. Ito, N. Tsuboya, D. Ooyama, N. Nagao, F.S. Howell, M. Mukaida, Inorg. Chim. Acta 290 (1999) 113;
(i) C.W.B. Bezerra, S.C. Silva, M.T.P. Gambardella, R.H.A. Santos, L.M.A. Plicas, E. Tfouni, D.W. Franco, Inorg. Chem. 38 (1999) 5660;
(j) D.H. Bohle, E.S. Sagan, Eur. J. Inorg. Chem. (2000) 1609.
[19] I.P. Evans, A. Spencer, W. Wilkinson, J. Chem. Soc. Dalton Trans. (1973) 204.
[20] J.E. Fergusson, C.T. Page, W.T. Robinson, Inorg. Chem. 15 (1976) 2270.
[21] R.K. Coll, J.E. Fergusson, V. McKee, C.T. Page, W.T. Robinson, T.S. Keong, Inorg. Chem. 26 (1987) 106.
[22] (a) J. Reedijk, Comments Inorg. Chem. 1 (1982) 379;
(b) I.B. Gorrell, G. Parkin, Inorg. Chem. 29 (1990) 2452.
[23] A.R. Davies, F.W.B. Einstein, N.P. Farrell, B.R. James, R.S. McMillan, Inorg. Chem. 17 (1978) 1965.
[24] (a) J.T. Veal, D.J. Hodgson, Inorg. Chem. 11 (1972) 1420;
(b) F. Bottomley, J. Chem. Soc. Dalton Trans. (1974) 1600;
(c) F. Bottomley, J. Chem. Soc. Dalton Trans. (1975) 2538.
[25] S. Geremia, M. Calligaris, J. Chem. Soc. Dalton Trans. (1997) 1541.
[26] M. Calligaris, O. Carugo, Coord. Chem. Rev. 153 (1996) 83.
[27] M. Haukka, M. Ahlgren, T.A. Pakkanen, J. Chem. Soc. Dalton Trans. (1996) 1927.
[28] R.W. Callahan, T.J. Meyer, Inorg. Chem. 16 (1977) 574.
[29] L.G.F. Lopes, M.G. Gomes, S.S.S. Borges, D.W. Francot, Aust. J. Chem. 51 (1998) 865.
[30] B. Mondal, H. Paul, V.G. Puranik, G.K. Lahiri, J. Chem. Soc. Dalton Trans. (2001) 481.
[31] A.B.P. Lever, Inorg. Chem. 29 (1990) 1271.
[32] D.W. Pipes, T.J. Meyer, Inorg. Chem. 23 (1984) 2466.